

Speed limit effect during lane change in a two-lane lattice model under V2X environment

Can Jin(金灿), Guang-Han Peng(彭光含), and Fang-Yan Nie(聂方彦)
Citation: Chin. Phys. B, 2024, 33 (**3**): 038902. DOI: 10.1088/1674-1056/ad0bf6
Journal homepage: http://cpb.iphy.ac.cn; http://iopscience.iop.org/cpb

What follows is a list of articles you may be interested in

A novel lattice model integrating the cooperative deviation of density and optimal flux under V2X environment

Guang-Han Peng(彭光含), Chun-Li Luo(罗春莉), Hong-Zhuan Zhao(赵红专), and Hui-Li Tan(谭惠丽)
Chin. Phys. B, 2023, 32 (**1**): 018902. DOI: 10.1088/1674-1056/ac65f1

A novel car-following model by sharing cooperative information transmission delayed effect under V2X environment and its additional energy consumption

Guang-Han Peng(彭光含), Te-Ti Jia(贾特提), Hua Kuang(邝华), Hui-Li Tan(谭惠丽), and Tao Chen(陈陶)
Chin. Phys. B, 2022, 31 (**5**): 058901. DOI: 10.1088/1674-1056/ac422a

CO_2 emission control in new CM car-following model with feedback control of the optimal estimation of velocity difference under V2X environment

Guang-Han Peng(彭光含), Rui Tang(汤瑞), Hua Kuang(邝华), Hui-Li Tan(谭惠丽), and Tao Chen(陈陶)
Chin. Phys. B, 2021, 30 (**10**): 108901. DOI: 10.1088/1674-1056/ac1417

Influence of bottleneck on single-file pedestrian flow: Findings from two experiments

Cheng-Jie Jin(金诚杰), Rui Jiang(姜锐), Da-Wei Li(李大韦)
Chin. Phys. B, 2020, 29 (**8**): 088902. DOI: 10.1088/1674-1056/ab8da3

A new cellular automaton model accounting for stochasticity in traffic flow induced by heterogeneity in driving behavior

Xiaoyong Ni(倪晓勇), Hong Huang(黄弘)
Chin. Phys. B, 2019, 28 (**9**): 098901. DOI: 10.1088/1674-1056/ab343b

---

Speed limit effect during lane change in a two-lane lattice model under V2X environment

Can Jin(金灿)[1,3], Guang-Han Peng(彭光含)[1,2,†], and Fang-Yan Nie(聂方彦)[4,‡]

[1] *College of Physical Science and Technology, Guangxi Normal University, Guilin* 541004, *China*
[2] *Guangxi Key Laboratory of Nuclear Physics and Technology, Guangxi Normal University, Guilin* 541004, *China*
[3] *Information and Modern Education Technology Center, Hunan University of Arts and Science, Changde* 415000, *China*
[4] *Computer and Information Engineering College, Guizhou University of Commerce, Guiyang* 550014, *China*

(Received 7 October 2023; revised manuscript received 1 November 2023; accepted manuscript online 13 November 2023)

Speed limit measures are ubiquitous due to the complexity of the road environment, which can be supplied with the help of vehicle to everything (V2X) communication technology. Therefore, the influence of speed limit on traffic system will be investigated to construct a two-lane lattice model accounting for the speed limit effect during the lane change process under V2X environment. Accordingly, the stability condition and the mKdV equation are closely associated with the speed limit effect through theory analysis. Moreover, the evolution of density and hysteresis loop is simulated to demonstrate the positive role of the speed limit effect on traffic stability in the cases of strong reaction intensity and high limited speed.

Keywords: traffic flow, lattice model, speed limit

PACS: 89.40.–a, 05.70.Fh **DOI:** 10.1088/1674-1056/ad0bf6

1. Introduction

With the increase of traffic flux, traffic problems are becoming more and more severe. Therefore, many scholars actively have engaged in traffic flow modeling research to investigate the underlying causes of traffic congestion. Currently, traffic micro models[1–13] and macro models[14–20] are advantageous in investigating traffic phenomena. Especially, Natagani[21–23] provided original lattice models to reproduce complex traffic phenomena on a single lane and two lanes, which can demonstrate the evolution process of traffic flux, density and speed. In recent years, many derivative models have successfully emerged since various traffic information factors were mined. These traffic factors are mainly connected with the differences of flux and density.[24–32] Also, the impact of traffic information in lattice models has been attracted by scholars, which covered the time delay,[33–38] the interruption probability,[39,40] the driver's anticipation[41–45] and others.[46–66] Moreover, the lane-changing phenomenon also attracts the interest of some scholars.[67–78] Recently, vehicle to everything (V2X) technology helps to enable the real-time transmission of traffic information. In an actual transportation environment, the slope, curve, narrow road and tunnel inevitably exist on the road, which require adopting a speed limit method to ensure traffic safety especially in lane changing situations. In addition, in the information coverage area, the speed limit requirements of roads can be shared as traffic information. And connected vehicles can use V2X communication technology to obtain the speed limit information, which contributes adopting corresponding reaction behaviors. But the speed limit effect (SLE) has not been surveyed under lane change. Subsequently, the SLE will be employed to fabricate a novel two-lane lattice model under V2X environment. Also, the effectiveness of the SLE will be proven through theoretical analysis and numerical simulation concerning density and hysteresis loop.

2. Construction of two-lane model integrating the speed limit effect

Figure 1 presents the lane change in the Nagatani's two-lane lattice model, integrating double continuity equations as follows:[3]

$$\begin{aligned}&\partial_t\rho_{1,j}+\rho_0(\rho_{1,j}v_{1,j}-\rho_{1,j-1}v_{1,j-1})\\&=\gamma\left|\rho_0^2V'(\rho_0)\right|(\rho_{2,j+1}-2\rho_{1,j}+\rho_{2,j-1}),\end{aligned}\tag{1}$$

$$\begin{aligned}&\partial_t\rho_{2,j}+\rho_0(\rho_{2,j}v_{2,j}-\rho_{2,j-1}v_{2,j-1})\\&=\gamma\left|\rho_0^2V'(\rho_0)\right|(\rho_{1,j+1}-2\rho_{2,j}+\rho_{1,j-1}),\end{aligned}\tag{2}$$

where $\rho_{i,j}$ represents the local density and $v_{i,j}$ is the local velocity. And ρ_0 is the average density. At site-j on lane 1, there appear the lane changing rate $\gamma\left|\rho_0^2V'(\rho_0)\right|(\rho_{2,j-1}-\rho_{1,j})$ under $\rho_{2,j-1}>\rho_{1,j}$ and $\gamma\left|\rho_0^2V'(\rho_0)\right|(\rho_{1,j}-\rho_{2,j+1})$ under $\rho_{1,j}>\rho_{2,j+1}$. Here γ is the rate constant coefficient. Consequently, making $\rho_j=(\rho_{1,j}+\rho_{2,j})/2$ and

$$\rho_jv_j=(\rho_{1,j}v_{1,j}+\rho_{2,j}v_{2,j})/2,$$

we integrate Eqs. (1) and (2) to get the continuity equation as follows:

$$\partial_t\rho_j+\rho_0(\rho_jv_j-\rho_{j-1}v_{j-1})$$

†Corresponding author. E-mail: pengguanghan@163.com
‡Corresponding author. E-mail: niefyan@gzcc.edu.cn

© 2024 Chinese Physical Society and IOP Publishing Ltd

$$= \gamma\left|\rho_0^2 V'(\rho_0)\right|(\rho_{j+1}-2\rho_j+\rho_{j-1}), \tag{3}$$

where $V'(\rho_0) = \mathrm{d}V(\rho)/\mathrm{d}t|_{\rho_0}$ and the optimal velocity $V(\rho)$ is employed as follows:

$$V(\rho) = \frac{v_{\max}}{2}\left[\tanh\left(\frac{2}{\rho_0}-\frac{\rho}{\rho_0^2}-\frac{1}{\rho_c}\right)+\tanh\left(\frac{1}{\rho_c}\right)\right], \tag{4}$$

where ρ_c indicates the safety density and $v_{\max}$ denotes the maximal speed. Additionally, the evolution equation is adopted as follows:

$$\partial_t(\rho_j v_j) = a\left[\rho_0 V(\rho_{j+1})-\rho_j v_j\right]. \tag{5}$$

Here a is the sensitivity coefficient. Nagatani's two-lane lattice model includes Eqs. (3) and (5). Subsequently, a number of extended two-lane lattice models[67–78] are concerned with different traffic factors. In modern transportation environments, transportation infrastructure is complex and dangerous roads often appear. Therefore, the speed limit method is an important measure to ensure safety, which will occur in the SLE. However, previous two-lane lattice models have not thought about the SLE during the evolution process. Accordingly, a new evolution equation is put forward by integrating the SLE under the V2X environment

$$\partial_t(\rho_j v_j) = a\left[\rho_0 V(\rho_{j+1})-\rho_j v_j\right]+\lambda a\left(\rho_j v_{\lim}-\rho_{j+1}v_{\lim}\right), \tag{6}$$

where $\lambda a(\rho_j v_{\lim}-\rho_{j+1}v_{\lim})$ indicates the SLE. $v_{\lim}$ and λ denote the limited velocity and the reaction coefficient. Blending Eqs. (3) and (6) with dissolving the velocity, one derives

$$\begin{aligned}&\rho_j(t+2\tau)-\rho_j(t+\tau)+\tau\rho_0^2\left[V(\rho_{j+1})-V(\rho_j)\right]\\&+\tau\rho_0\lambda v_{\lim}\left[(\rho_j-\rho_{j+1})-(\rho_{j-1}-\rho_j)\right]-\tau\gamma\left|\rho_0^2V'(\rho_0)\right|\\&\times\left[\rho_{j+1}(t+\tau)-2\rho_j(t+\tau)+\rho_{j-1}(t+\tau)\right]=0,\end{aligned} \tag{7}$$

where $\tau = 1/a$ expresses the delay time.

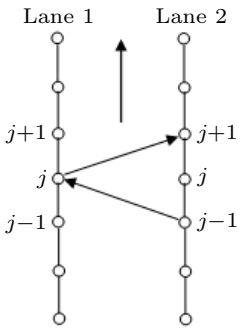


Fig. 1. The schematic model of traffic flow on two lanes.

3. Linear stability analysis

Firstly, $y_j(t)$ is defined as a small deviation as follows:

$$\rho_j(t) = \rho_0 + y_j(t). \tag{8}$$

Then, Eq. (7) can be replaced by

$$\begin{aligned}&y_j(t+2\tau)-y_j(t+\tau)+\tau\rho_0^2V'(\rho_0)(y_{j+1}-y_j)\\&+\tau\rho_0\lambda v_{\lim}\left[(y_j-y_{j-1})-(y_{j+1}-y_j)\right]-\tau\gamma\left|\rho_0^2V'(\rho_0)\right|\\&\times\left[y_{j+1}(t+\tau)-2y_j(t+\tau)+y_{j-1}(t+\tau)\right]=0.\end{aligned} \tag{9}$$

Making $y_j = A\exp(\mathrm{i}kj+zt)$, one attains

$$\begin{aligned}&\mathrm{e}^{2z\tau}-\mathrm{e}^{z\tau}+\tau\rho_0^2V'(\rho_0)(\mathrm{e}^{\mathrm{i}k}-1)\\&+\tau\rho_0\lambda v_{\lim}\left[(1-\mathrm{e}^{-\mathrm{i}k})-(\mathrm{e}^{\mathrm{i}k}-1)\right]\\&-\tau\gamma\left|\rho_0^2V'(\rho_0)\right|\left(\mathrm{e}^{\mathrm{i}k+z\tau}-2\mathrm{e}^{z\tau}+\mathrm{e}^{-\mathrm{i}k+z\tau}\right)=0.\end{aligned} \tag{10}$$

Moreover, putting $z = z_1(\mathrm{i}k)+z_2(\mathrm{i}k)^2+\cdots$ into Eq. (10), we deduce

$$z_1 = -\rho_0^2V'(\rho_0), \tag{11}$$

$$z_2 = -\frac{\rho_0^2V'}{2}-\gamma\rho_0^2V'+\lambda v_{\lim}\rho_0-\frac{3(\rho_0^2V')^2\tau}{2}. \tag{12}$$

Finally, a balanced traffic flow is maintained when $z_2 > 0$. As $z_2 < 0$, the uniform flow falls conversely into an unstable state. Accordingly, the unstable condition is deduced as

$$\tau > -\frac{(1+2\gamma)\rho_0^2V'-2\lambda v_{\lim}\rho_0}{3(\rho_0^2V')^2}. \tag{13}$$

Correspondingly, one gets the neutral stability condition as

$$\tau = -\frac{(1+2\gamma)\rho_0^2V'-2\lambda v_{\lim}\rho_0}{3(\rho_0^2V')^2}. \tag{14}$$

Accordingly, we fulfil the neutral stability curve as shown in Fig. 2 (the solid line). Here $v_{\max} = 2$, $\gamma = 0.05$ and $v_{\lim} = 0.8v_{\max}$. Obviously, the stable range gradually magnifies with the reaction coefficient of SLE amplifying.

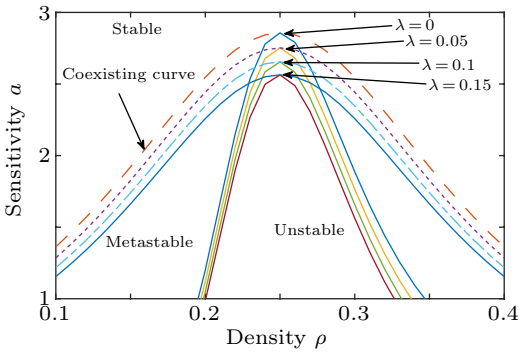


Fig. 2. The phase diagram in parameter space (ρ, a).

4. Nonlinear analysis

To begin with, we define a small variable ε for the following variables X and T with a constant b:

$$X = \varepsilon(j+bt), \quad T = \varepsilon^3 t. \tag{15}$$

Moreover, the density is adopted by

$$\rho_j = \rho_c + \varepsilon R(X,T). \tag{16}$$

Here $R(X,T)$ implies a function involving X and T. Consequently, we can expand Eq. (7) to quintic power by variable ε as follows:

$$\begin{aligned}&\varepsilon^2(b+\rho_c^2V')\partial_X R+\varepsilon^3\left[\frac{3b^2\tau}{2}-\lambda v_{\lim}\rho_c+\frac{1+2\gamma}{2}\rho_c^2V'\right]\partial_X^2R\\&+\varepsilon^4\left[\partial_T R+\left(\frac{7b^3\tau^2}{6}+\frac{\rho_c^2V'}{6}+\gamma b\rho_c^2V'\tau\right)\partial_X^3R+\frac{\rho_c^2V'''}{6}\partial_X R^3\right]\\&+\varepsilon^5\Bigg[3b\tau\partial_T\partial_X R+\left(\frac{5b^4\tau^3}{8}+\frac{\rho_c^2V'}{24}-\frac{1}{12}\lambda v_{\lim}\right.\\&\left.+\frac{\gamma\rho_c^2V'}{12}+\frac{\gamma\rho_c^2V'(b\tau)^2}{2}\right)\partial_X^4R+\frac{\rho_c^2V'''}{12}\partial_X^2R^3\Bigg]=0,\end{aligned}\tag{17}$$

where $V'=\mathrm{d}V(\rho)/\mathrm{d}\rho|_{\rho=\rho_c}$ and $V'''=\mathrm{d}^3V(\rho)/\mathrm{d}\rho^3\big|_{\rho=\rho_c}$. Moreover, Eq. (17) can be simplified with $\tau/\tau_c=1+\varepsilon^2$ and $b=-\rho_c^2V'$,

$$\begin{aligned}&\varepsilon^4(\partial_T R-h_1\partial_X^3R+h_2\partial_X R^3)\\&+\varepsilon^5(h_3\partial_X^2R+h_4\partial_X^4R+h_5\partial_X^2R^3)=0.\end{aligned}\tag{18}$$

Here

$$h_1=-\frac{1}{6}\left[\rho_c^2V'-\frac{14\lambda v_{\lim}-7\rho_cV'^2}{9\rho_c^2V'^2}\right]+\gamma b\rho_c^2V'\tau_c,\tag{19a}$$

$$h_2=\frac{\rho_c^2V'''}{6},\quad h_3=\lambda v_{\lim}\rho_c-(1+\gamma)\frac{\rho_c^2V'}{2},\tag{19b}$$

$$\begin{aligned}h_4=&-\frac{1}{24}\left[3\rho_c^2V'-6\lambda v_{\lim}\rho_c+\frac{23(2\lambda v_{\lim}-\rho_cV')^3}{9\rho_cV'^2}\right]\\&+\frac{\gamma\rho_c^2V'}{12}\left[6(b\tau_c)^2+1\right],\end{aligned}\tag{19c}$$

$$h_5=\frac{\rho_c^2V'''}{12}\left(1+\frac{4\lambda v_{\lim}-2\rho_cV'}{\rho_cV'}\right).\tag{19d}$$

Accordingly, one expresses the following propagation velocity v:

$$v=5h_2h_3/(2h_2h_4-3h_1h_5).\tag{20}$$

Consequently, the kink–antikink soliton solution is described by

$$\begin{aligned}\rho_j(t)=&\rho_c+\sqrt{\frac{h_1v}{h_2}\left(\frac{\tau}{\tau_c}-1\right)}\tanh\sqrt{\frac{v}{2}\left(\frac{\tau}{\tau_c}-1\right)}\\&\times\left[j+\left(1-vh_1\left(\frac{\tau}{\tau_c}-1\right)\right)t\right].\end{aligned}\tag{21}$$

Obviously, the amplitude D is conveyed as

$$D=\sqrt{\frac{h_1v}{h_2}\left(\frac{\tau}{\tau_c}-1\right)}.\tag{22}$$

Thereupon, the coexisting curves are displayed in Fig. 2 (dashed curves) based on $\rho_j=\rho_c\pm D$. Then, one sees three regions of the phase diagram covering the stable region, the metastable region and the unstable region, which states that the neutral and the coexisting curves fall down due to the SLE amplifying.

5. Numerical simulation

In this section, the periodic boundary condition is applied and the initial conditions are employed as

$$\begin{cases}\rho_j(0)=\rho_j(1)=\rho_0+0.1, & j=50,\\ \rho_j(0)=\rho_j(1)=\rho_0-0.1, & j=51,\\ \rho_j(0)=\rho_j(1)=\rho_0, & \text{others}.\end{cases}\tag{23}$$

First of all, the spatiotemporal evolution of density waves is described at different $v_{\lim}$ as shown in Fig. 3, corresponding density profiles displayed in Fig. 4 at 10300 time step, where $N=100$, $\rho_0=0.25$, $\gamma=0.05$, and $a=2.58$. According to Figs. 3 and 4, the amplitude of density waves magnifies as the limited speed decreases and the kink–antikink density wave occurs in Figs. 3(a)–3(c), which reveals that the lower limited speed will deteriorate the stability of traffic flow.

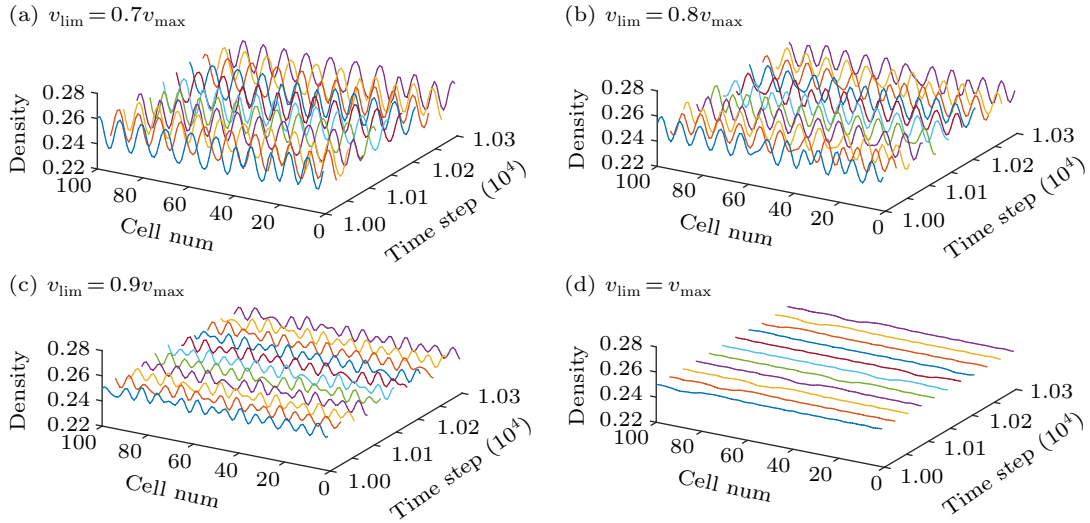


Fig. 3. The spatiotemporal evolution of density waves for different $v_{\lim}$.

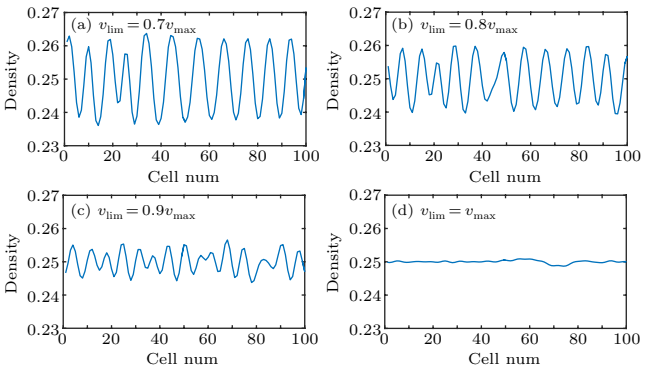


Fig. 4. The density profiles at 10300 time step corresponding to Fig. 3.

Moreover, the three dimensional density evolution is exhibited for different reaction coefficients λ in Fig. 5. And Fig. 6 represents the density profiles related to Fig. 5 at the 10300th time step for all sites, where $v_{\rm lim}=0.8v_{\rm max}$. From Figs. 5 and 6, the density vibration lessens by amplifying λ-value, which states that traffic jam can be effectively restrained by ascending the intensity of the SLE in two-lane system. Also, a stable state has emerged in Figs. 5(d) and 6(d) as $\lambda=0.12$, which demonstrates that the SLE promotes the stability of two-lane traffic flow.

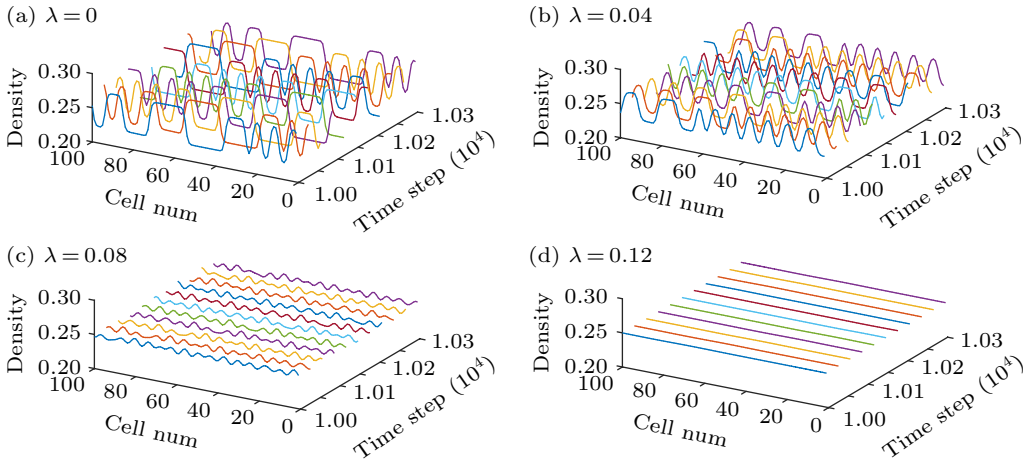


Fig. 5. The spatiotemporal evolution of density waves for different λ.

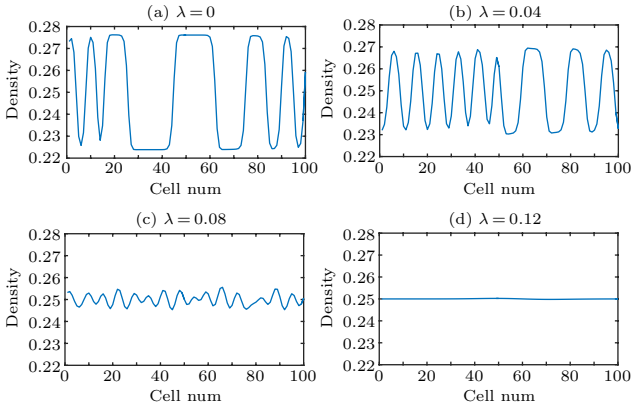


Fig. 6. The density profiles at 10300 time step for different λ corresponding to Fig. 5.

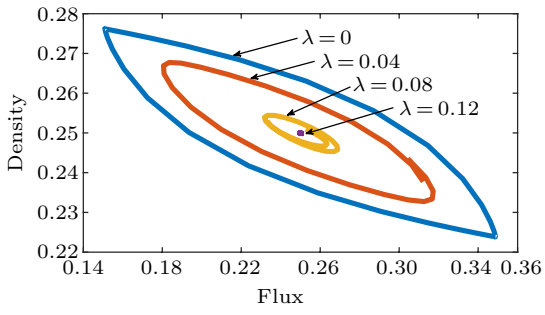


Fig. 7. The hysteresis loop of the 55th lattice between flux and density.

Finally, due to the asynchronous flow and density during the acceleration and deceleration processes of the traffic flow, a hysteresis loop phenomenon occurs. Therefore, we get hold of the hysteresis loop according to flux and density displayed in Fig. 7. Observing Fig. 7, the hysteresis loop obviously shrinks by enlarging the λ-value, which certificates that the SLE contributes to the stable situation of two-lane traffic system. Moreover, as $\lambda=0.12$, the hysteresis loop vanishes owing to the stable state of two-lane traffic flow in this case.

6. Conclusion

Due to road bottlenecks, it is often necessary to limit the speed of vehicles for safety reasons. Accordingly, V2X communication is adopted to convey information of the speed limit effect in building two-lane lattice model. Also, we obtain the stability condition closely related to the speed limit effect on two lanes. Moreover, nonlinear analysis is performed to derive the mKdV equation connected with the speed limit effect. Additionally, it is confirmed that the speed limit effect can be applied to suppress traffic congestion with the advantage of the two-lane freeway. Consequently, it is completely necessary to consider the speed limit effect in traffic flow modeling on two lanes. Surely, how to consider a reasonable speed limit range based on the physical conditions of traffic roads is an interesting topic in future research.

Acknowledgments

Project supported by the Guangxi Natural Science Foundation, China (Grant No. 2022GXNSFDA035080), the Central Government Guidance Funds for Local Scientific and Technological Development, China (Grant No. Guike ZY22096024), and the National Natural Science Foundation, China (Grant No. 61963008).

References

[1] Zhai C, Wu W T and Luo S W 2021 *Chin. Phys. B* **30** 100507
[2] Zeng J W, Qian Y S, Li J, Zhang Y Z and Xu D J 2023 *Physica A* **609** 128331
[3] Wang X, Xue Y and Feng S W 2023 *Eur. Phys. J. B* **96** 85
[4] Zhang F T, Qian Y S and Zeng J W 2023 *IEEE Trans. Intell. Transp. Syst.* **24** 6507
[5] Zhai C and Wu W 2018 *Nonlinear Dyn.* **93** 2185
[6] Zhai C and Wu W 2021 *Nonlinear Dyn.* **106** 3379
[7] Zhai C, Wu W and Xiao Y 2022 *Appl. Math. Model.* **108** 770
[8] Ren W L, Cheng R J and Ge H X 2021 *Chin. Phys. B* **30** 120506
[9] Gong Y and Zhu W X 2022 *Chin. Phys. B* **31** 024502
[10] Yadav S and Redhu P 2023 *Nonlinear Dyn.* **111** 13245
[11] Zhang X Z, Shi Z K, Yu S W and Ma L J 2023 *Physica A* **615** 128551
[12] Peng G H, Wang K K, Zhao H Z and Tan H L 2023 *Nonlinear Dyn.* **111** 13089
[13] Han Y Y, Bai C C, Jin S, Wang R J and Ma D F 2023 *Transp. B* **11** 1311
[14] Zhai C and Wu W 2018 *Phys. Lett. A* **382** 3381
[15] Zhai C and Wu W 2021 *Physica A* **584** 126364
[16] Zhai C and Wu W 2022 *Physica A* **588** 126561
[17] Jiang Y Q, Hu Y G and Huang X Q 2022 *Physica A* **608** 128272
[18] Zhang G and Tian D D 2021 *Chin. Phys. B* **30** 120201
[19] Zhai C, Wu W T and Xiao Y P 2023 *Chaos Solitons Fractals* **171** 113515
[20] Peng G H, Luo C L, Zhao H Z and Tan H L 2023 *Chin. Phys. B* **32** 018902
[21] Nagatani T 1998 *Physica A* **261** 599
[22] Nagatani T 1999 *Physica A* **264** 581
[23] Nagatani T 1999 *Physica A* **265** 297
[24] Tian J, Jia B, Li X and Gao Z 2010 *Chin. Phys. B* **19** 040303
[25] Wang T, Gao Z, Zhao X, Tian J and Zhang W 2012 *Chin. Phys. B* **21** 070507
[26] Li Z P, Li X L and Liu F Q 2008 *Int. J. Mod. Phys. C* **19** 1163
[27] Tian J, Yuan Z, Jia B, Li M and Jiang G 2012 *Physica A* **391** 4476
[28] Wang T, Gao Z, Zhang J and Zhao X 2014 *Nonlinear Dyn.* **75** 27
[29] Gupta A and Redhu P 2014 *Commun. Nonlinear Sci. Numer. Simulat.* **19** 1600
[30] Tian C, Sun D and Zhang M 2011 *Commun. Nonlinear Sci. Numer. Simul.* **16** 4524
[31] Redhu P and Gupta A 2014 *Nonlinear Dyn.* **78** 957
[32] Gupta A and Redhu P 2013 *Phys. Lett. A* **377** 2027
[33] Ge H X, Zheng P J, Lo S M and Cheng R J 2014 *Nonlinear Dyn.* **76** 441
[34] Kang Y R and Sun D H 2013 *Nonlinear Dyn.* **71** 531
[35] Zhang Y, Wang S, Pan D B and Zhang G 2021 *Physica A* **561** 125269
[36] Ren X and Zhao S 2021 *Nonlinear Dyn.* **103** 1869
[37] Wang Q, Cheng R J and Ge H X 2020 *Physica A* **559** 125023
[38] Chang Y, He Z and Cheng R 2019 *Physica A* **514** 522
[39] Redhu P and Gupta A 2015 *Physica A* **421** 249
[40] Zhai C and Wu W 2019 *Mod. Phys. Lett. B* **33** 1950273
[41] Sharma S 2015 *Nonlinear Dyn.* **81** 991
[42] Gupta A and Redhu P 2013 *Physica A* **392** 5622
[43] Gupta A and Redhu P 2014 *Nonlinear Dyn.* **76** 1001
[44] Kaur R and Sharma S 2018 *Physica A* **499** 110
[45] Wang T, Zang R, Xu K and Zhang J 2019 *Physica A* **526** 120711
[46] Zhang Y, Zhao M, Sun D, Wang S, Huang S and Chen D 2021 *Commun. Nonlinear Sci. Numer. Simul.* **94** 105541
[47] Zhai C and Wu W 2021 *Commun. Nonlinear Sci. Numer. Simul.* **95** 105667
[48] Ge H X, Cui Y, Zhu K Q and Cheng R J 2015 *Commun. Nonlinear Sci. Numer. Simul.* **22** 903
[49] Redhu P and Gupta A 2015 *Commun. Nonlinear Sci. Numer. Simul.* **27** 263
[50] Li Y F, Zhang L, Zheng T X and Li Y G 2015 *Commun. Nonlinear Sci. Numer. Simul.* **29** 224
[51] Zhu C Q, Zhong S Q, Li G Y and Ma S F 2017 *Physica A* **468** 445
[52] Zhou J and Shi Z 2016 *Nonlinear Dyn.* **83** 1217
[53] Gupta A, Sharma S and Redhu P 2014 *Commun. Theor. Phys.* **62** 393
[54] Cheng R and Wang Y 2019 *Physica A* **513** 510
[55] Zhang G 2018 *Nonlinear Dyn.* **91** 809
[56] Zhang G, Sun D H and Zhao M 2018 *Commun. Nonlinear Sci. Numer. Simul.* **54** 347
[57] Jiang C, Cheng R J and Ge H X 2019 *Physica A* **513** 465
[58] Redhu P and Siwach V 2018 *Physica A* **492** 1473
[59] Verma M and Sharma S 2022 *Chaos Solitons Fractals* **162** 112435
[60] Gupta A, Sharma S and Redhu P 2015 *Nonlinear Dyn.* **80** 1091
[61] Natagani T 1999 *Phys. Rev. E* **60** 1535
[62] Zhang Y C, Zhao M and Sun D H 2022 *Physica A* **603** 127710
[63] Kaur R and Sharma S 2018 *Physica A* **510** 446
[64] Sharma S 2016 *Nonlinear Dyn.* **86** 2093
[65] Kaur R and Sharma S 2017 *Physica A* **471** 59
[66] Kaur R and Sharma S 2018 *Phys. Lett. A* **382** 1449
[67] Li Z P, Zhang R, Xu S Z and Qian Y Q 2015 *Commun. Nonlinear Sci. Numer. Simul.* **24** 52
[68] Zhang G, Sun D H and Liu W N 2015 *Nonlinear Dyn.* **81** 1623
[69] Zhang G, Sun D H, Liu W N, Zhao M and Cheng S L 2015 *Physica A* **422** 16
[70] Zhang G, Sun D H, Zhao M, Liu W N and Cheng S L 2015 *Int. J. Mod. Phys. C* **26** 1550062
[71] Sharma S 2015 *Physica A* **421** 401
[72] Zhu C Q, Zhong S Q and Ma S F 2019 *Commun. Nonlinear Sci. Numer. Simul.* **73** 229
[73] Madaan N and Sharma S 2021 *Physica A* **564** 125446
[74] Madaan N and Sharma S 2022 *Physica A* **599** 127393
[75] Sun F, Chow A, Lo S M and Ge H X 2018 *Physica A* **511** 389
[76] Zhai C and Wu W 2018 *Mod. Phys. Lett. B* **32** 1850233
[77] Madaan N and Sharma S 2022 *Eur. Phys. J. B* **95** 6
[78] Wang T, Zhang J, Gao Z Y, Zhang W Y and Li S B 2017 *Nonlinear Dyn.* **88** 1345